Computers & Fluids 106 (2015) 12–18

Contents lists available at ScienceDirect

Computers & Fluids

journal homepage: www.elsevier.com/locate/compfluid

On the numerical technique for the simulation of hypervelocity test flows

Z.M. Hu [a,*], C. Wang [a], Z.L. Jiang [a], B.C. Khoo [b,c]

[a] State Key Laboratory of High-temperature Gas Dynamics (LHD), Institute of Mechanics, Chinese Academy of Sciences, Beijing 100190, China
[b] Department of Mechanical Engineering, National University of Singapore, 119260 Singapore, Singapore
[c] Temasek Laboratories, National University of Singapore, 117411 Singapore, Singapore

ARTICLE INFO

Article history:
Received 31 March 2013
Received in revised form 6 September 2014
Accepted 15 September 2014
Available online 30 September 2014

Keywords:
Hypervelocity test flow
DCD scheme
Flux-splitting
Spurious oscillation

ABSTRACT

A shock-expansion tube (SET) is one of the major ground test facilities to generate really high-enthalpy and hypervelocity test flows. However, the strong shock wave may give rise to chemically non-equilibrium characteristic flow feature in a SET. In addition, the test time duration of a SET is extremely short which leads to difficulties in measurements and flow diagnostics. It is therefore appropriate to consider employing CFD approach, coupled with available experimental data, to determine the characteristic of the test flow in a SET. The dispersion-controlled dissipative scheme (DCD) is used for our simulation of chemically non-equilibrium flows associated with a SET. In this paper, the several numerical issues which occur in the computational investigation of the test flow in our SET facility are discussed. A new flux splitting algorithm based on local characteristics is worked out for the DCD scheme to mitigate any spurious oscillations. With the mentioned updated DCD scheme, the computed results compare well with the experimental data provided for validation.

1. Introduction

Reflected shock tunnels (RST) are the main workhorse ground test facilities for the study of hypersonic flow. However, severe challenges arise when the RSTs are used for hypervelocity experiments where the test flow velocity may exceed 5 km/s. The contamination of the test gas and material erosion of the nozzle reservoir are severe issues among others which may lead to uncertainties of the prevailing test flow conditions. A shock-expansion tube (SET) has the potential to mitigate the aforementioned concerns to a certain extent and generate relatively clean test gas of very high enthalpy and hypervelocity because the test flow is not stagnated anywhere. A series of SETs have been set up around the world, e.g., X-2 and X-3 at the Queensland University [1–4], HYPULSE at GASL [5], LENS-X at CUBRC [6], JX-1 in Japan [7,8], a SET of low-speed range for the investigation of scramjet at Stanford University [9–11], and others [12]. A detonation-driven SET has been built at the State Key Laboratory of High Gas Dynamics (LHD) and has successfully generated hypervelocity test flows of up to 8 km/s and beyond [13,14]. However, the test duration of the SET is extremely short as compared to a RST of the same length scale which leads to difficulties in measurements and flow diagnostics. Generally, the test times and test flow properties are estimated via available measurements, e.g., static and pitot pressure measurements, spectral emission measurements [8] and others.

Due to the inherent difficulties in relying on experiments, it is therefore reckoned appropriate to consider CFD techniques, coupled with available experimental measurement, to determine the characteristic of the test flow in a SET. Jacobs [15] first used perfect gas model and laminar flow simulation to study the test flow properties of X-2 and further included the finite-rate chemical kinetics and strong viscous effects in the expansion tube for the simulation of SET X-3 [16]. The turbulent boundary layer in the expansion tube was simulated [17] in conjunction with the HYPULSE facility. It was reported in recent studies that the growth of turbulent boundary layer in the expansion tube is a critical issue limiting the test time of a shock-expansion tube [4,11]. The major objective of relevant computational investigations is to estimate the test time and test flow properties of the ground-based hypervelocity facilities [11,18]. However, it has been a great challenge to simulate and capture the essence of the complex flow dynamic phenomena in the SET, especially contributed by the chemically and thermally non-equilibrium effects under such high-enthalpy conditions. In addition, according to the nature of extremely short running time of a SET test facility, simulation can hardly be properly validated due to the lack of available test data.

* Corresponding author. Tel.: +86 10 8254 5812; fax: +86 10 8254 3996.
E-mail addresses: huzm@imech.ac.cn (Z.M. Hu), mpekbc@nus.edu.sg (B.C. Khoo).

http://dx.doi.org/10.1016/j.compfluid.2014.09.039
0045-7930/

In the present study, a numerical scheme called dispersion-controlled dissipative (DCD), is modified to simulate the hypervelocity test flow in the detonation-driven SET located at LHD. The original DCD scheme was proposed by Jiang intending for shock wave capturing [19,20]. The primary principle of the scheme aims at keeping free of any spurious oscillations at strong discontinuities by a limiter reflecting the dispersion condition of the modified equation. The DCD scheme, without any tunable parameters, avoids encountering the 'carbuncle' phenomena altogether even for the case of very strong shock wave. It has also been successfully applied to chemically reacting flows for compressible multi-component mixtures [21–25] and flows in the presence of strong shock wave interaction [26,27]. The mentioned applications have attested to the DCD scheme as fairly robust, computationally efficient, and capable of resolving strong discontinuities. However, non-physical oscillation can still occur when the original DCD scheme is used to simulate the hypervelocity test flow in our preliminary computations. In the present paper, a new term of numerical flux is formed for the modified DCD scheme, which can eliminate the aforementioned oscillation. The hypervelocity test flow conditions are then analyzed and validated by comparison with experiments.

2. Governing equations

In the present study, we focus on the overall test flow property of the SET without considering the boundary layer at the tunnel walls and the thermally non-equilibrium effects. In other words, the essence of the paper is on the deployment of effective numerical technique for capturing the resultant strong shock waves under the auspices of chemical nonequilibrium associated with high enthalpy, high temperature and hypervelocity. In 2D Cartesian coordinates, the conservative form of the multi-component chemically reacting Euler equation is written as:

$$\frac{\partial U}{\partial t}+\frac{\partial F}{\partial x}+\frac{\partial G}{\partial y}=S_c \quad (i=1,2). \tag{1}$$

Here, U is the unknown variable vector, F and G are the inviscid flux vectors in the x and y directions, respectively, and Sc is the source term of the chemical reaction, where

$$U=[\rho C_1,\ldots,\rho C_{ns},\rho u,\rho v,\rho e] \tag{2}$$

$$F=[\rho C_1 u,\ldots,\rho C_{ns}u,\rho u^2+p,\rho uv,(\rho e+p)u] \tag{3}$$

$$G=[\rho C_1 v,\ldots,\rho C_{ns}v,\rho uv,\rho v^2+p,(\rho e+p)v] \tag{4}$$

$$S_c=[\dot{\omega}_1,\ldots,\dot{\omega}_{ns},0,0,0,0]. \tag{5}$$

In the above equations, the density of the mixture is $\rho=\sum_{sp=1}^{ns}\rho_{sp}=\sum_{sp=1}^{ns}\rho C_{sp}$, where the mass fraction and the partial density of the species sp is denoted by C_{sp} and ρ_{sp}, respectively. u and v are the velocity components in the x and y directions. $e=\rho h-p+\frac{1}{2}\rho(u^2+v^2)$ denotes the total energy per unit volume, where $h=\sum_{sp=1}^{ns}C_{sp}h_{sp}$ and p are the enthalpy and pressure of the mixture, respectively. $\dot{\omega}_{sp}$ is the rate of change of the species sp due to chemical reaction. The thermodynamic properties of each species, i.e., the special heat capacity and enthalpy h_{sp}, are obtained from relations given in the power series form of temperature [28]. The detailed chemical kinetic model consists of seventeen elementary reactions among the following five species, i.e., N_2, O_2, NO, O and N.

3. The original DCD scheme for multi-component system

The attractive feature of the DCD scheme is that it can aptly manage the scheme numerical dissipation according to the discontinuity intensity to maintain stability without introducing any free parameters which are generally problem dependant. More details on the DCD scheme can be found in the review work [20].

The original second-order DCD scheme for the convective part of Eq. (1) in two-dimensional Cartesian coordinates (x,y) can be written as follows,

$$\left(\frac{\partial \mathbf{U}}{\partial t}\right)_{ij}=-\frac{1}{\Delta x}\left(\overline{\mathbf{F}}_{i+\frac{1}{2}}-\overline{\mathbf{F}}_{i-\frac{1}{2}}\right)_j-\frac{1}{\Delta y}\left(\overline{\mathbf{G}}_{j+\frac{1}{2}}-\overline{\mathbf{G}}_{j-\frac{1}{2}}\right)_i, \tag{6}$$

where the numerical flux term, $\overline{\mathbf{F}}_{i+\frac{1}{2}}$, for the scheme can be obtained by the following equations,

$$\overline{\mathbf{F}}_{i+\frac{1}{2}}=\mathbf{F}^+_{i+\frac{1}{2}}+\mathbf{F}^-_{i+\frac{1}{2}} \tag{7}$$

$$\mathbf{F}^+_{i+\frac{1}{2}}=\mathbf{F}^+_i+\frac{1}{2}minmod(\mathbf{F}^+_i-\mathbf{F}^+_{i-1},\mathbf{F}^+_{i+1}-\mathbf{F}^+_i) \tag{8}$$

$$\mathbf{F}^-_{i+\frac{1}{2}}=\mathbf{F}^-_i-\frac{1}{2}minmod(\mathbf{F}^-_{i+2}-\mathbf{F}^-_{i+1},\mathbf{F}^-_{i+1}-\mathbf{F}^-_i). \tag{9}$$

The term $\overline{\mathbf{G}}$ is similar to that of $\overline{\mathbf{F}}$ and is not given here for brevity. It can be seen from Eqs. (7)–(9) that the split fluxes, $\mathbf{F}^{\pm}_m$, at the nodes $(m=i-1,i,i+1,i+2)$ are required to calculate the numerical flux $\overline{\mathbf{F}}_{i+\frac{1}{2}}$. The characteristic-based splitting algorithm is written as

$$\mathbf{F}^{\pm}_m=(\mathbf{R}\Lambda^{\pm}\mathbf{L})_m\mathbf{U}_m, m=i-1,i,i+1,i+2. \tag{10}$$

Here, $\mathbf{R},\mathbf{L}$ and Λ are the right, left eigenvectors and the eigenvalue diagonal matrix of the Jacobian, $\mathbf{A}=\partial\mathbf{F}/\partial\mathbf{U}$, respectively. As the flow variables at the same node are used for the calculation of $\mathbf{R},\mathbf{L},\Lambda$ and $\mathbf{U}$ the split fluxes $\mathbf{F}^{\pm}_m$ for the original DCD scheme [19,20] may be manipulated in a simplified form,

$$\mathbf{F}^{\pm}_m=\frac{\rho}{2\gamma}\begin{bmatrix} C_1[2(\gamma-1)\lambda^{\pm}_1+\lambda^{\pm}_{ns+2}+\lambda^{\pm}_{ns+3}] \\ \vdots \\ C_{ns}[2(\gamma-1)\lambda^{\pm}_1+\lambda^{\pm}_{ns+2}+\lambda^{\pm}_{ns+3}] \\ u[2(\gamma-1)\lambda^{\pm}_1]+(u-c)\lambda^{\pm}_{ns+2}+(u+c)\lambda^{\pm}_{ns+3} \\ v[2(\gamma-1)\lambda^{\pm}_1]+(v-c)\lambda^{\pm}_{ns+2}+(v+c)\lambda^{\pm}_{ns+3} \\ 2[(\gamma-1)H-c^2]\lambda^{\pm}_1+(H-c)\lambda^{\pm}_{ns+2}+(H+c)\lambda^{\pm}_{ns+3} \end{bmatrix}. \tag{11}$$

Here, $\lambda^{\pm}_i=\frac{1}{2}(\lambda_i\pm\sqrt{\lambda_i^2+\varepsilon}), \quad (i=1,2,\ldots,ns+3, \quad 0<\varepsilon\ll 1)$ while λ_i is the eigenvalues of the Jacobian, i.e., the diagonal elements of Λ. For the Jacobian A of the multi-component system, the eigenvalues are as follows

$$\lambda_{i,1\leqslant i\leqslant ns+1}=u; \quad \lambda_{ns+2}=u; \quad \lambda_{ns+3}=u-c. \tag{12}$$

In the above equations, $H=h+0.5(u^2+v^2)$ is the total enthalpy of the mixture per unit mass and c is the frozen speed of sound of the mixture.

As given in Eqs. (7)–(11), the numerical flux for the DCD scheme can be calculated explicitly in a straightforward means. Therefore, it is very easy for coding and computationally cheap since the matrix operation is not needed. Our computational experience indicates that the DCD scheme is robust for shock wave capturing. Fig. 1 (left), for instance, shows the carbuncle problem generally appears when an upwind scheme is used. Entropy correction with a tunable parameter is introduced to the TVD scheme [29] which can eliminate the carbuncle phenomenon. However, the aforementioned DCD scheme is proved to be free of instability without any case-by-case tunable parameter as shown in Fig. 1 (right). The DCD scheme has been applied to simulate shock wave problems in inert or reacting flows [21–27]. However, serious spurious oscillation occurs when the original DCD scheme is used for the simulation of hypervelocity test flow in the detonation-driven expansion tube, JF-16 [13,14].

The configurations of geometry and wave process of the shock-expansion tube JF-16 is schematically shown in Fig. 2. There are two diaphragms which divide the facility into three sections, i.e.,

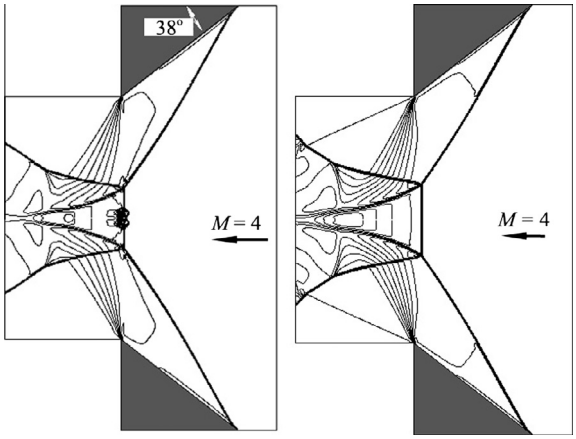

Fig. 1. DCD scheme and the carbuncle problem, Left: TVD [29], Right: DCD [19].

the detonation tube, shock tube and acceleration tube. After the detonation wave has impacted and crashed the diaphragm I, the primary shock wave (psw) is generated in the shock tube followed by the primary contact surface (pcs) that separates the driver gases and the driven gas. In a reflected shock tunnel (RST), the driven gas is stagnated at the nozzle which results in erosion and contamination due to high temperature. On the contrary, the psw along with the driven gas in a SET moves downstream into the accelerating tube after breaking the diaphragm II. The driven gas is further accelerated through the unsteady expansion (uex) to generate the test flow in the Zone No. 5 (see Fig. 2). In short, the test flow in a SET is never stagnated which consequently avoid any contamination and erosion as found inevitably in a RST test facility.

For the test condition at total enthalpy of around 45 MJ/kg, the detonation tube is filled with hydrogen and oxygen at pressure of $p_4 = 1.5$ MPa, while the shock tube and acceleration tube are vacuumized to $p_1 = 3990$ Pa and $p_7 = 13.3$ Pa, respectively. Here, the subscripts $_{1,4,7}$ represent the initial filling conditions of the different sections of the JF-16 test facility (see Fig. 2 for more details). The Mach number of psw wave in the shock tube and secondary shock wave (ssw) in the expansion tube are $M_{psw} = 13.9$ and $M_{ssw} = 23$, respectively, according to the measurements from the Run No. 22 of JF-16 [30]. It is found that the static temperature is sufficiently high to cause dissociation of air post the strong shock wave of psw or ssw, respectively. As such, a chemical reaction model should be applied in the present simulation which consists of seventeen elementary reactions among five species, i.e., N_2, O_2, NO, O and N.

In the following simulation, only the flow in the shock tube and acceleration tube as demonstrated and shown in the dashed-box in Fig. 2 is simulated. Therefore, the incident shock wave, i.e., psw, in the shock tube should be predetermined for the initial condition according to the experiment data while the detonation tube is not simulated. As depicted in Fig. 3, we can see spurious oscillations in the profiles at the second contact surface (scs) where the original DCD scheme is used for the case of total enthalpy of 45 MJ/kg. For this case, the velocity of the test flow is around 8.8 km/s which exceeds the orbital speed. Why does the scheme work well in previous simulations [21–25] of chemically reactive flow but lead to spurious oscillation in the present simulation?

4. The updated DCD scheme for hypervelocity test flow simulation

One can see a sharp jump of temperature across the second contact surface (scs) as shown in Fig. 3. Such a temperature gradient consequently leads to a sharp gradient of thermodynamic properties, the speed of sound and chemical kinetics. The simulation using the original DCD scheme for the case of a lower total enthalpy, i.e., 14 MJ/kg which corresponds to a test flow velocity of 6.4 km/s, as depicted in Fig. 4 gives a reasonable solution without any spurious oscillation. In this case, the temperature jump across the contact surface is not so intense as that for the case of 45 MJ/kg. For the setup of the simulation for 14 MJ/kg, parameters are kept the same as for the higher enthalpy case except that $p_7 = 3.0$ mmHg. By adjusting p_7 we can obtain different test flow velocities of JF-16. Numerical tests using the original DCD scheme show that spurious oscillation occurs when $p_7 \leqslant 0.5$ mmHg corresponding to a total enthalpy $H_t \geqslant 18$ MJ/kg. For a characteristic-based flux-split scheme like DCD, the very sharp gradient may generally cause numerical instabilities, for instance, the previous

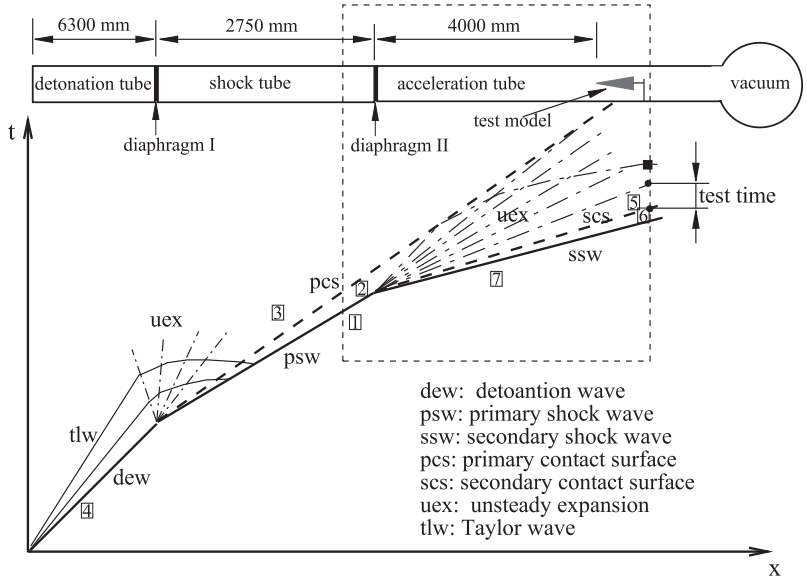

Fig. 2. Sketch of the configuration and wave graph for JF-16 shock-expansion tube. (The numbers in the boxes represent different flow conditions, e.g., 1: pre-psw or the initial filling conditions in the shock tube, 2: post-psw or the driven gas, 3: post-pcs or the driver gas, 4: initial filling condition in the detonation tube, 5: post-scs or the test flow in the acceleration tube, 6: post-ssw or the accelerated gas, 7: pre-ssw or the initial filling condition in the acceleration tube, respectively.)

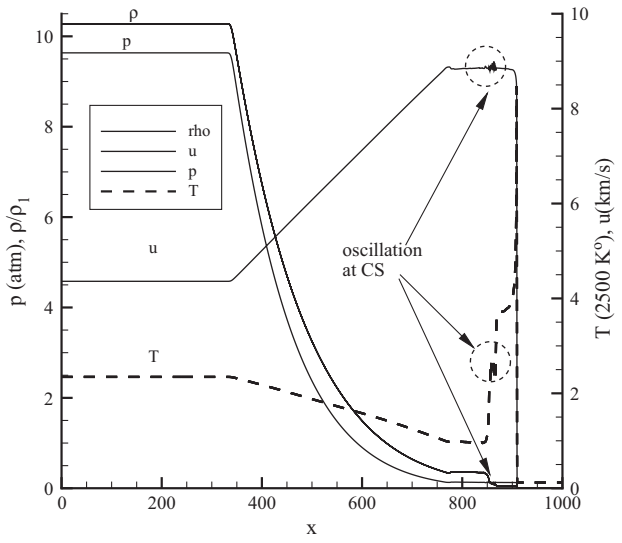

Fig. 3. Spurious oscillation in the simulation of JF-16 at total enthalpy of 45 MJ/kg with the original DCD scheme.

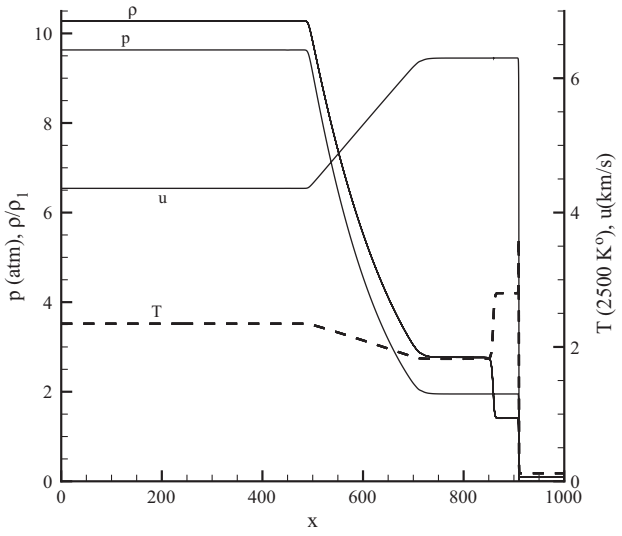

Fig. 4. Simulation of JF-16 at total enthalpy of 14 MJ/kg with the original DCD scheme.

simulation of flow supercavitation using DCD scheme [31]. The flux splitting algorithm for the original DCD scheme is schematically shown in Fig. 5 where the numerical flux can be written as

$$\overline{\mathbf{F}}^{o}_{i+\frac{1}{2}} = \mathbf{F}^{+}_{i} + \mathbf{F}^{-}_{i+1} + \frac{1}{2}minmod(\mathbf{F}^{+}_{i} - \mathbf{F}^{+}_{i-1}, \mathbf{F}^{+}_{i+1} - \mathbf{F}^{+}_{i}) - \frac{1}{2}minmod(\mathbf{F}^{-}_{i+1} - \mathbf{F}^{-}_{i}, \mathbf{F}^{-}_{i+2} - \mathbf{F}^{-}_{i+1}). \quad (13)$$

It can be seen from Fig. 5 and Eq. (13) that the characteristic parameters at grid nodes $(i-1, i, i+1, i+2)$ are required to calculate the split flux $\mathbf{F}^{\pm}_{m}$ (Eq. (11)) respectively, and finally get the numerical flux $\overline{\mathbf{F}}^{o}_{i+\frac{1}{2}}$ at the cell center $i+1/2$ for the original DCD scheme.

For the numerical simulation of multi-component compressible flows, spurious oscillations may occur at a contact discontinuity when there is a jump in both temperature and specific heat ratio across the discontinuity [32]. A quasi conservative approach was proposed by Abgrall to suppress the spurious oscillations [33] followed by a series of advanced techniques [34,35] among others. Although the DCD scheme [19,20] was originally proposed as a non-oscillation shock capturing scheme, unfortunately, it still admits spurious oscillation across the contact discontinuity with a severe parameter jump in the present study. In order to avoid the oscillation problem as depicted in Fig. 3, a modified DCD scheme is worked out and shall be shown to be able to capture well the second contact surface. The flux splitting algorithm as written in Eq. (14) for the modified DCD scheme is schematically shown in Fig. 6. It can be clearly seen that only the local eigenvectors, $\mathbf{R}_{1+1/2}$ and $\mathbf{L}_{1+1/2}$, and the eigenvalue, $\Lambda^{\pm}_{i+1/2}$, at the cell center $(i+\frac{1}{2})$ are required for the numerical flux $\overline{\mathbf{F}}^{U}_{i+\frac{1}{2}}$. That is,

$$\overline{\mathbf{F}}^{U}_{i+\frac{1}{2}} = \mathbf{R}_{1+1/2}\left[\mathbf{f}^{+}_{i} + \mathbf{f}^{-}_{i+1} + \frac{1}{2}minmod(\mathbf{f}^{+}_{i} - \mathbf{f}^{+}_{i-1}, \mathbf{f}^{+}_{i+1} - \mathbf{f}^{+}_{i}) - \frac{1}{2}minmod(\mathbf{f}^{-}_{i+1} - \mathbf{f}^{-}_{i}, \mathbf{f}^{-}_{i+2} - \mathbf{f}^{-}_{i+1})\right], \quad (14)$$

where the intermediate flux is

$$\mathbf{f}^{\pm}_{m} = (\Lambda^{\pm}\mathbf{L})_{i+1/2}\mathbf{U}_{m}, (m = i-1, i, i+1, i+2). \quad (15)$$

For the original DCD scheme as depicted in Fig. 5, variables at the same node are used to calculate the characteristic vectors, i.e., $\mathbf{R}, \Lambda^{\pm}, \mathbf{L}$, and the unknown vector, i.e., $\mathbf{U}$. Therefore, the split flux $\mathbf{F}^{\pm}_{m} = (\mathbf{R}\Lambda^{\pm}\mathbf{L})_{m}\mathbf{U}_{m}, (m = i-1, i, i+1, i+2)$ for the original DCD scheme can be manually simplified via matrix manipulation to obtain a compact term as given in Eq. (11). The original DCD scheme is easy for programming and computationally cheap due to the aforementioned simplicity which has been used successfully in a series of applications [21–27] except the simulation of shock-expansion tube running at high enthalpy. For the updated DCD scheme, however, the flow variables used for calculating the eigenvectors and eigenvalues are different from those used for the unknown vector as can be seen from Eq. (15) and Fig. 6. Therefore, Eq. (15) cannot be further simplified and its calculation becomes more computational expensive than the original DCD scheme.

The calculated profiles using the modified DCD scheme for hypervelocity flow of total enthalpy of 45 MJ/kg are depicted in

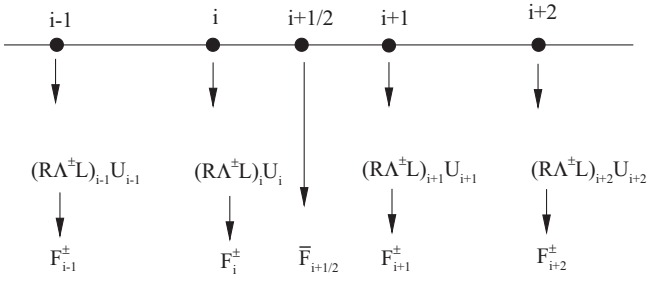

Fig. 5. Sketch of the flux splitting algorithms for the original DCD scheme.

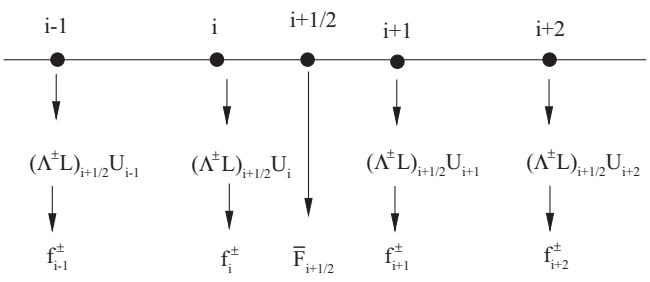

Fig. 6. Sketch of the flux splitting algorithms for the updated DCD scheme.

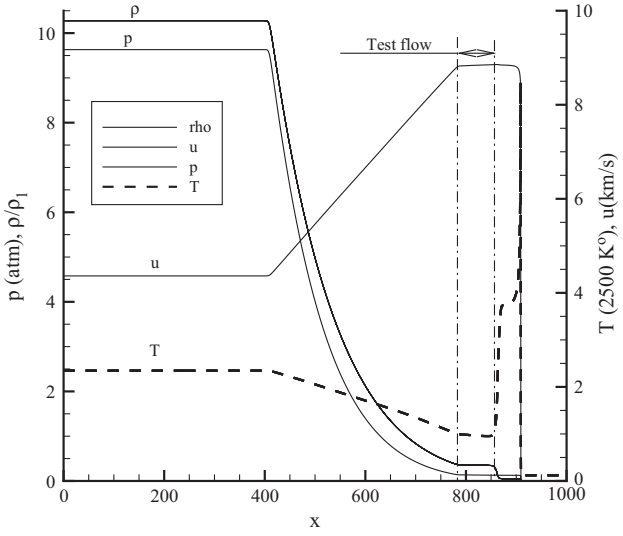

Fig. 7. Simulation of JF-16 at total enthalpy of 45 MJ/kg with the updated DCD scheme.

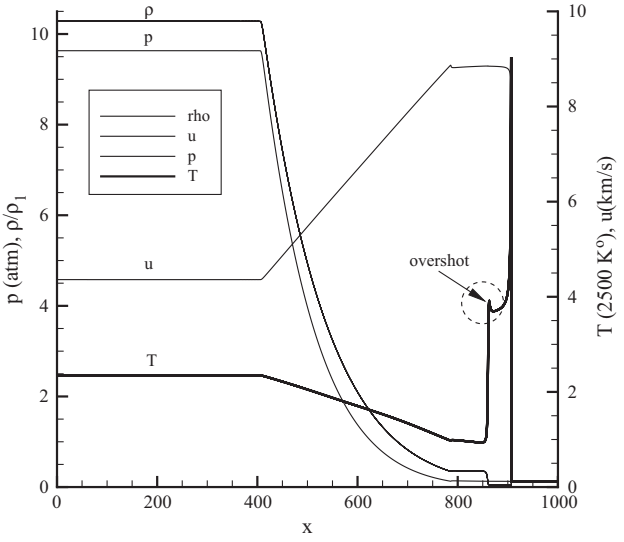

Fig. 9. Simulation of JF-16 at total enthalpy of 45 MJ/kg with WENO scheme [36].

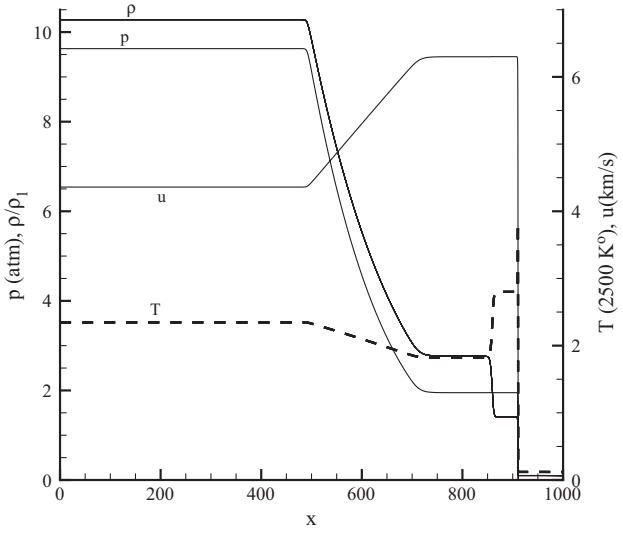

Fig. 8. Simulation of JF-16 at total enthalpy of 14 MJ/kg with the updated DCD scheme.

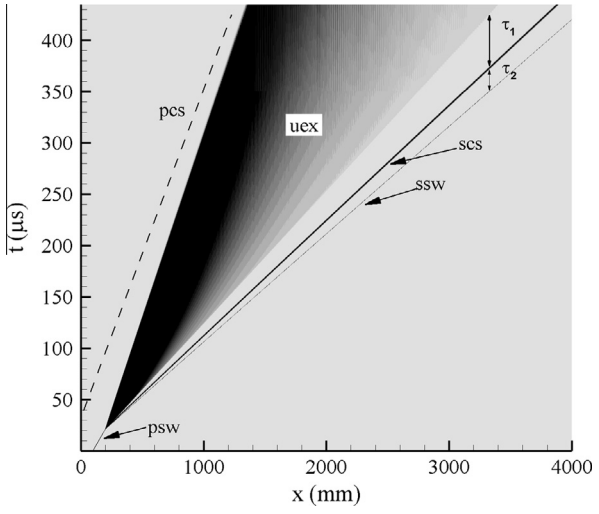

Fig. 10. The wave-diagram of JF-16 at total enthalpy of 45 MJ/kg.

Fig. 7 where there is no longer the spurious oscillations in the vicinity of the second contact surface. As demonstrated in Fig. 8, the modified DCD scheme also works well for the lower enthalpy case of 14 MJ/kg and gives identical solution as plot in Fig. 4 which is simulated by the original DCD scheme.

The hypervelocity test flow at total enthalpy of 45 MJ/kg is additionally simulated using the WENO scheme [36]. As shown in Fig. 9, the WENO scheme does resolve well the contact surface when compared to the updated DCD simulation as given in Fig. 7. Instead, an overshot problem at the contact surface occurs as marked by the dashed circle in Fig. 9. Except for the aforementioned differences, the overall parameters associated with the test flow conditions respectively calculated with the updated DCD scheme and the WENO scheme agree well with each other.

5. Numerical simulation for test models

The calculated wave diagram is shown in Fig. 10 for the hypervelocity test flow with a total enthalpy of 45 MJ/kg. The diagram corresponds to the figure segment enclosed in the dashed box in Fig. 2 which shows the primary wave phenomena in the acceleration tube downstream of diaphragm II. The test time duration of JF-16, the flow time τ_1 of Zone No. 5, is 60 μs as obtained by the simulation. The extremely short duration leads to difficulties in test flow diagnosis and measurements. Therefore, numerical simulation is an essential means to approximately evaluate the test flow conditions, e.g., the static pressure $p_5 = 0.13$ atm, temperature $T_5 = 2600$ K, and velocity $u_5 = 8.8$ km/s for the high enthalpy case. Under such conditions, the molecular oxygen in the test flow is mostly dissociated while molecular nitrogen survives according to the simulation. As such, the JF-16 shock-expansion tube, at its current status, cannot reproduce the chemical composition for a real hypervelocity free-stream flow. It can simulate the velocity of above the orbital speed but cannot duplicate the Mach number due to the high temperature of the test flow. A divergent nozzle is therefore needed to further cool down the test gas through steady expansion according to the plan of upgrading the test facility in the future.

Presently, we have carried out model tests for the different geometries like wedge, cone and double-cone as shown in

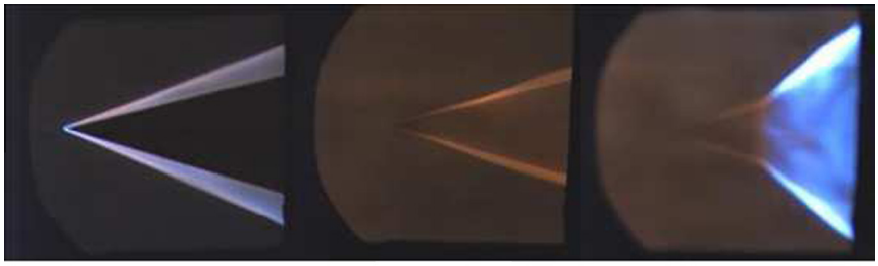

Fig. 11. Experimental model tests in JF-16 at total enthalpy of 45 MJ/kg: (a) wedge with half angle of 15°; (b) cone with half angle of 15°; and (c) double-cone geometry with half angle of 15° + 35°.

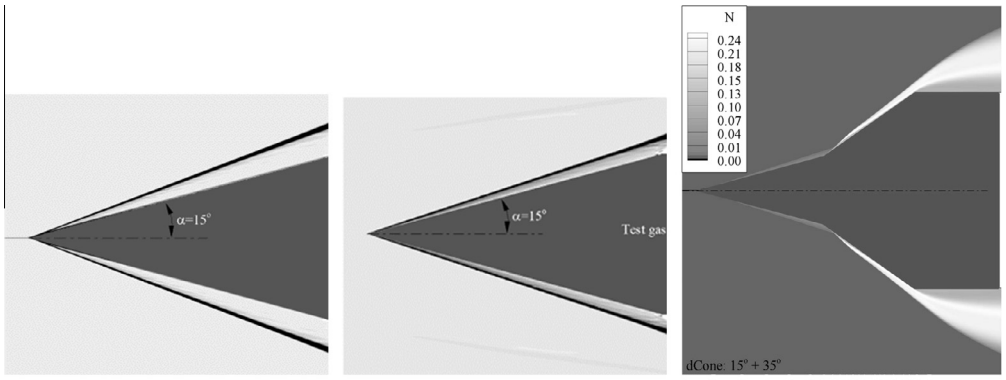

Fig. 12. Simulation of test model in JF-16 at total enthalpy of 45 MJ/kg: (a) schlieren over a wedge with half angle of 15°; (b) schlieren over a cone with half angle of 15°; and (c) atomic nitrogen distribution over a double-cone geometry with half angle of 15° + 35°.

Fig. 11. The images were taken by a high-speed camera for the self-illumination of the main species in the test flow which can show the shock wave structure over the geometries. Here, the exposure time of the camera is 1 μs while the frame frequency is 40 kHz. In the tests, the initial conditions of the test facility are as follows, (1) The detonation tube is filled with hydrogen–oxygen mixture at pressure of p_4 = 1.5 MPa while the volume ratio is 1:4; (2) The shock tube is filled with air at pressure of p_1 = 3990 Pa; and (3) Air in the acceleration tube is at pressure of p_7 = 13.3 Pa. All the gases are at room temperature, i.e., $T_4 = T_1 = T_7 = 300$ K. As such, a hypervelocity test flow of total enthalpy about 45 MJ/kg can be obtained for the model tests.

An interesting phenomenon is the color change across the shock wave as can be seen in each frame of Fig. 11. Despite the same test flow condition, the post-shock gas appears light blue, yellow and bright blue in frame (a)–(c), respectively. Accordingly, numerical simulations are conducted and shown in Fig. 12 for the aforementioned model tests. The first two frames are for schlieren images and the third is the distribution of atomic nitrogen, i.e., N. The shock wave structures shown in Figs. 11(a) and (b) and 12(a) and (b) agree well with each other. For the case of double-cone geometry as shown in Fig. 12(c), the simulated distribution contours of other species such as O_2, N_2, NO and O are not consistent with the experimental image as depicted in Fig. 11(c). As such, we can deduce that the images taken in experiment are for the self-illumination of species N.

As aforementioned, the test flow consists of molecular nitrogen and atomic oxygen according to the numerical simulation. For the test model of double-cone geometry, the first oblique shock wave over the first cone surface is not strong enough to significantly dissociate the molecular nitrogen which leads to light color region downstream the first oblique shock wave. Due to the larger inclination angle 35°, however, the second oblique shock wave over the second cone surface becomes sufficiently strong to generate more atomic nitrogen which hence results in a brighter region as depicted in Figs. 11(c) and 12(c). Based on this investigation, we can now interpret the color difference between the post-shock flowfield in Fig. 11(a) and (b) respectively of the wedge and cone. Theoretically, the oblique shock wave over a wedge is stronger than that over a cone with the same inclination angle. Consequently, more N_2 can be dissociated into N within the post-shock region of Fig. 11(a) than (b). Therefore, the color of post-shock region as shown in Fig. 11(a) is slightly brighter than that as depicted in Fig. 11(b). Numerical computations also confirm the above findings.

6. Conclusions

In the present study, we modified the dispersion-controlled-dissipative (DCD) scheme for the simulation of hypervelocity test flow in a shock-expansion tube (SET). Spurious oscillation can be mitigated by using the new numerical technique. Due to the extremely short test time duration and the critical non-equilibrium phenomena, test flow diagnostics becomes very difficult in the SET experiments. Therefore, we have to indirectly analyze the test flow conditions by means of computational fluid dynamics. We found via computations that the self-illumination color is associated with the dissociation degree of nitrogen post the oblique shock wave over each studied test model. Numerical simulations also indicate that the test facility needs further improvement to simulate the chemical composition and Mach number for real hypervelocity test flows.

Acknowledgement

The work is supported by the National Natural Science Foundation of China under Grant Nos. 11142006 and 90916028.

References

[1] Morgan RG, Stalker RJ. Double diaphragm driven expansion tube. In: 18th International symposium on shock waves. Sendai, Japan; 1991.
[2] Morgan RG. Development of X3, a superorbital expansion tube. In: 38th Aerospace sciences meeting and exhibit. AIAA paper 2000–0558; 2000.
[3] Scott MP. Development and modelling of expansion tubes, PhD thesis. University of Queensland, St. Lucia, Australia; 2006.
[4] McGilvray M. Scramjet testing at high enthalpies in expansion tube facilities, PhD thesis. University of Queensland, St. Lucia, Australia; 2008.
[5] Chue RSM, Tsai CY, Bakos RJ, Erdos JI, Rogers RC. Advanced hypersonic test facilities, Progress in Astronautics and Aeronautics, vol. 198. AIAA; 2002 [chapter 3: NASA's HYPULSE Facility at GASL: A Dual Mode, Dual Driver Reflected-Shock/Expansion Tunnel].
[6] Holden MS, Wadhams TP, MacLean M, Mundy E. Experimental studies in the LENS I and X to evaluate real gas effects on hypervelocity vehicle performance. In: 45th AIAA aerospace sciences meeting and exhibit. Reno, Nevada, AIAA paper 2007–204; January 2007.
[7] Sasoh A, Ohnishi K, Koremoto K, Takayama K. Operation design and performance of a free piston driven expansion tube. In: 37th AIAA aerospace sciences meting and exhibition. Reno, Nevada, AIAA paper 99-0825, January 1999.
[8] Sasoh A, Ohnishi Y, Ramjam D, Takayama K, Otsu H, Abe T. Effective of test time evaluation in high-enthalpy expansion tube. AIAA J 2001;39(11):2141–7.
[9] Ben-Yakar A, Hanson RK. Characterization of expansion tube flows for hypervelocity combustion studies. J Prop Power 2002;18(4):943–51.
[10] Heltsley WN, Snyder JA, Houle AJ, Davidson DF, Mungal MG, Hanson RK. Design and characterization of the standard 6 inch expansion tube. AIAA Paper 2006-4443, AIAA Aerospace Sciences Meeting; 2006.
[11] Orley F, Strand CL, Miller VA, Gamba M, Adams NA, Iaccarino G. A study of expansion tube gas flow conditions for scramjet combustor model testing. Center Turbul Res Annu Res Briefs 2011:285–96.
[12] Dufrene A, Sharma M, Austin JM. Design and characterization of a hypervelocity expansion tube facility. In: 45th AIAA aerospace sciences meeting. AIAA paper 2007–1327; January 2007.
[13] Jiang ZL, Gao YL, Zhao W. Performance study on detonation-driven expansion tube. In: 16th AIAA/DLR/DGLR international space planes and hypersonic systems and technologies conference. Bremen, Germany; October 2009.
[14] Gao YL. Study on hypervelocity flow generation techniques and essential hypersonic phenomena, PhD thesis. Beijing, China: Institute of Mechanics, CAS; 2008.
[15] Jacobs PA. Numerical simulation of transient hypervelocity flow in an expansion tube. Comput Fluids 1994;23(1):77–101.
[16] Jacobs PA, Silvester TB, Morgan RG, Scott MP, Gollan RJ, McIntyre TJ. Superorbital expansion tube operation: estimates of flow conditions via numerical simulation. In: 43rd AIAA aerospace sciences meeting. AIAA paper 2005–694; January 2005.
[17] Wilson GJ, Sussman MA, Bakos RJ. Numerical simulations of the flow in the HYPULSE expansion tube. NASA TM-110357; June 1995.
[18] Otsu H, Abe T, Ohnishi Y, Sasoh A, Takayama K. Numerical investigation of high-enthalpy flows generated by expansion tube. AIAA J 2002;40(12):2423–30.
[19] Jiang ZL, Takayama K, Chen YS. Dispersion conditions for non-oscillatory shock-capturing schemes and its applications. Comput Fluid Dyn J 1995;2:137–50.
[20] Jiang ZL. On the dispersion-controlled principles for non-oscillatory shock-capturing schemes. Acta Mech Sin 2004;20:1–15.
[21] Hu ZM, Jiang ZL. Wave dynamic process in cellular detonation reflection from wedges. Acta Mech Sin 2007;23:33–41.
[22] Hu ZM, Dou HS, Khoo BC. Rapid detonation initiation by sparks in a short duct: a numerical study. Shock Waves 2010;20:241–9.
[23] Deng B, Hu ZM, Teng HH, Jiang ZL. Numerical study on cellular structure evolution of detonation in section-changing chambers. Sci China Ser G 2007;50(6):797–808.
[24] Hu ZM, Lv JM, Jiang ZL, Myong RS, Cho TH. Numerical study on the off-design/on-design performance of nozzle flow for supersonic chemical oxygen-iodine lasers. Acta Mech Sin 2008;24(2):133–42.
[25] Hu ZM, Jiang ZL, Myong RS, Cho TH. Numerical analysis of spatial evolution of the small signal gain in a chemical oxygen-iodine laser operating without primary buffer gas. Opt Laser Tech 2008;40(1):13–20.
[26] Hu ZM, Myong RS, Kim MS, Cho TH. Downstream flow conditions effects on the RR → MR transition of asymmetric shock waves in steady flows. J Fluid Mech 2009;620:43–62.
[27] Hu ZM, Wang C, Zhang Y, Myong RS. Computational confirmation of an abnormal Mach reflection wave configuration. Phys Fluids 2009;21:011701.
[28] McBride BJ, Zehe MJ, Sanford Gordon. NASA Glenn coefficients for calculating thermodynamic properties of individual species. NASA/TP 2002-211556, Glenn Research Center, Cleveland, Ohio; 2002.
[29] Yee HC, Klopfer GH, Montagne JL. High-resolution shock-capturing schemes for inviscid and viscous hypersonic flows. J Comput Phys 1990;88:31–61.
[30] Wu B. Study on the interaction of strong shock wave and the hypervelocity experimental method, PhD thesis. Beijing, China: Institute of Mechanics, CAS; 2012.
[31] Hu ZM, Dou HS, Khoo BC. On the modified dispersion-controlled dissipative (DCD) scheme for computation of flow supercavitation. Comput Fluids 2011;40:315–23.
[32] Karni S. Multicomponent flow calculations by a consistent primitive algorithm. J Comput Phys 1994;112:31–43.
[33] Abgrall R. How to prevent pressure oscillations in multicomponent flow calculations: a quasi conservation approach. J Comput Phys 1996;125:150–60.
[34] Fedkiw R, Liu XD, Osher S. A general technique for eliminating spurious oscillations in conservative schemes for multiphase and multispecies Euler equations. Int J Nonlinear Sci Numer Sim 2002;3:99–106.
[35] Hiroshi T, Soshi K, Mitsuo K. Approach to prevent spurious oscillation in compressible multicomponent flows using high-order methods ASME 2012 Fluids Engineering division summer meeting, vol. 1. Symposia, Parts A and B, Puerto Rico, USA; July 8–12, 2012.
[36] Jiang GS, Shu CW. Efficient implementation of weighted ENO schemes. J Comp Phys 1996;126:202–28.